Influence of the Counterion and Co−Ion Diffusion Coefficient Values on Some Dielectric and Electrokinetic Properties of Colloidal Suspensions

J. J. López-García,[†] C. Grosse,[‡,§] and J. Horno*[,†]

Departamento de Física, Universidad de Jaén, Campus de Las Lagunillas Ed. A3, 23071, Jaén, Spain, Departamento de Física, Universidad Nacional de Tucumán, Av. Independencia 1800, 4000 San Miguel de Tucumán, Argentina, and Consejo Nacional de Investigaciones Científicas y Técnicas, Argentina

Received: February 22, 2005; In Final Form: April 25, 2005

The dependences of the conductivity increment, the electrophoretic mobility, and the permittivity increment on the counterion diffusion coefficient value were numerically determined. The use of the network simulation method made it possible to solve the governing equations for the whole range of counterion and co-ion diffusion coefficients and for very low frequencies, despite the far-reaching field-induced charge density outside the double layer. Calculations performed for different ζ potential and electrolyte concentration values show that increasing the counterion mobility, while keeping constant the electrolyte solution conductivity and the κa values, strongly increases the conductivity increment, barely affects the electrophoretic mobility, and strongly decreases the permittivity increment. The numerical results are discussed and compared to analytical predictions derived from the Shilov−Dukhin model, which generally leads to a good agreement, at least for high κa and moderate ζ.

Introduction

Electrokinetic and dielectric properties are powerful analytical tools in colloidal science, being often used for the characterization of colloidal systems.[1−3] This is why theoretical models relating these phenomena to the system parameters have been developed in the last century. Among the studied systems, dilute suspensions of rigid spherical particles in suspension have a special significance, since they constitute the first approximation to real colloidal suspensions. However, even in this simplest case, analytical solutions only exist for some limiting cases, i.e., when the Debye length is much smaller or greater than particle radius, or when the ζ potential is small.[1,4−7]

Because of this, a number of numerical methods have been presented,[8−12] and used to analyze the dependence of electrokinetic properties on the ζ potential and on the electrolyte solution concentration. However, dependencies on other parameters of the system have not yet been analyzed in depth. For example, it is usual to assume that the diffusion coefficient values of counterions and co-ions are similar or equal. Nevertheless, recent works[13−16] show that, whenever these values differ, important modifications arise with respect to the simplest case of equal diffusion coefficients. The aim of this work is to analyze the influence of the diffusion coefficient values on the conductivity increment, the electrophoretic mobility, and the dielectric increment.

Basic Equations

We consider a charged nonconducting spherical particle of radius a and absolute permittivity ϵ_i, immersed in an ionic solution of permittivity ϵ_e, viscosity η, containing two types of monovalent ions with diffusion coefficients $D^{\pm}$ and volume concentration C_∞ far from any particle. The equations governing the dynamics of the system are well-known:[10]

(i) Nernst−Planck equations for the ionic flows:

$$\vec{J}^{\pm}(\vec{r},t) = -D^{\pm}\nabla C^{\pm}(\vec{r},t) \mp \frac{eD^{\pm}}{kT}C^{\pm}(\vec{r},t)\nabla\Phi(\vec{r},t) + C^{\pm}(\vec{r},t)\vec{v}(\vec{r},t) \quad (1)$$

(ii) Conservation equation for each ionic species:

$$\nabla\cdot\vec{J}^{\pm}(\vec{r},t) = -\frac{\partial C^{\pm}(\vec{r},t)}{\partial t} \quad (2)$$

(iii) Poisson equation:

$$\nabla^2\Phi(\vec{r},t) = -\frac{e[C^{+}(\vec{r},t) - C^{-}(\vec{r},t)]}{\epsilon_e} \quad (3)$$

(iv) Continuity equation for an incompressible fluid:

$$\nabla\cdot\vec{v}(\vec{r},t) = 0 \quad (4)$$

(v) Navier−Stokes equation for a viscous fluid:

$$\eta\nabla^2\vec{v}(\vec{r},t) - \nabla P(\vec{r},t) = e[C^{+}(\vec{r},t) - C^{-}(\vec{r},t)]\nabla\Phi(\vec{r},t) + \rho_f\left\{[\vec{v}(\vec{r},t)\cdot\nabla]\vec{v}(\vec{r},t) + \frac{\partial\vec{v}(\vec{r},t)}{\partial t}\right\} \quad (5)$$

where $C^{\pm}$ are the concentrations of the two types of ions ($C^{\pm}(r\to\infty, t) = C_\infty$), Φ is the electric potential, $\vec{J}^{\pm}$ are the ion flows, $\vec{v}$ is the fluid velocity, P is the pressure, $\vec{r}$ is the position vector, t is the time variable, and ρ_f is the mass density of the suspending medium.

The equation system is solved considering first the equilibrium situation. The solution to the nonequilibrium problem is then obtained considering that the applied field $E(t)$ is sufficiently weak so that all of the equations can be linearized with respect to E. Finally, a set of boundary conditions is used to determine the integration constants. This procedure is presented in detail in refs 17 and 18.

* To whom correspondence should be addressed.
[†] Universidad de Jaén.
[‡] Universidad Nacional de Tucumán.
[§] Consejo Nacional de Investigaciones Científicas y Técnicas.

10.1021/jp050918i CCC: $30.25
Published on Web 05/26/2005

The numerical calculations were performed using the network simulation method, which consists of modeling the governing differential equations by means of an electrical circuit that is analyzed by means of a circuit simulation program. Over the past few years, this method has been successfully applied to a variety of problems, including ionic transport in both membranes and electrochemical cells,[19] and nonequilibrium phenomena in colloidal suspensions.[17,18] A full account of the network model used in this work is given in ref 12, and a more general explanation of the method is given in ref 20.

In the present case, the Network Simulation method made it possible to solve the problem considering the full range of counterion and co-ion mobilities and for the very low frequencies required for the calculation of zero-frequency (as opposed to static) properties such as the conductivity and the permittivity increments. Under these conditions, the applied field induces electric charge densities that extend to great distances beyond the double layer,[16] which greatly increases the difficulties of the numerical calculations.

Results and Discussion

To discuss our results we are going to use the Shilov-Dukhin model,[1] which proved to be very successful for the interpretation of the low-frequency dielectric dispersion and the low-frequency electrorotation. It is based on the thin double layer approximation ($\kappa a \gg 1$) and also uses the hypothesis of quasiequilibrium inside the double layer and of approximate electroneutrality outside it. In the case of univalent electrolytes, it leads to the following expressions for the field-induced electrolyte concentration and electric potential changes outside the double layer:[21]

$$\frac{\delta(C^+ + C^-)}{2C_\infty} = K_c \frac{e^{-(1+i)W(r/a-1)}}{r^2/a^2} \frac{1+(1+i)Wr/a}{1+W+iW} \frac{eEa}{kT} \cos\theta \tag{6}$$

$$\delta\tilde{\Phi} = \left(\frac{K_d a^2}{r^2} - \frac{r}{a}\right)\frac{eEa}{kT}\cos\theta + \frac{\delta(C^+ + C^-)}{2C_\infty}\Delta \tag{7}$$

In these expressions

$$W = \sqrt{\frac{\omega a^2}{2D_{ef}}} \tag{8}$$

$$D_{ef} = \frac{2D^+D^-}{D^+ + D^-} \tag{9}$$

$$\Delta = \frac{D^- - D^+}{D^+ + D^-} \tag{10}$$

$$\tilde{\Phi} = \frac{e\Phi}{kT} \tag{11}$$

whereas K_c and K_d are frequency dependent integration coefficients: K_c is proportional to the variation of electrolyte concentration on the surface of the particle (calculated using expressions valid outside the thin double layer and extrapolated up to $r = a$), and K_d is proportional to the induced dipole moment of the suspended particle. The above results have the following important properties:

1. For any finite frequency value, the electrolyte concentration change decreases exponentially with distance, so that the dipolar term of the electric potential is determined by the coefficient $K_d(\omega)$.

2. For a static field ($\omega = 0$), the exponential in eq 6 reduces to unity so that the electrolyte concentration change becomes dipolar. Therefore, the dipolar coefficient acquires an additional term

$$K_{dstatic} = K_d(0) + K_c(0)\Delta \tag{12}$$

3. For $r = a$ the exponential in eq 6 also reduces to unity. Therefore, both for the low-frequency limit and for a static field, the electric potential extrapolated to the surface of the particle is given by

$$\delta\tilde{\Phi} = [K_d(0) + K_c(0)\Delta - 1]\frac{eEa}{kT}\cos\theta \tag{13}$$

The final expressions for the integration coefficients, obtained using boundary conditions, are[21]

$$K_c = \frac{3(R^+ - R^-)}{2}\frac{1+W+iW}{iW^2A + (1+W+iW)B} \tag{14}$$

$$K_d = K_{d\infty} - K_c H \tag{15}$$

where

$$A = R^+(1-\Delta) + R^-(1+\Delta) + 4 \tag{16}$$

$$B = \frac{(R^+ + 2)(R^- + 2 - U^-) + (R^- + 2)(R^+ + 2 - U^+)}{2} \tag{17}$$

$$K_{d\infty} = \frac{R^+(1-\Delta) + R^-(1+\Delta) - 2}{A} \tag{18}$$

$$H = \frac{(R^+ - R^-)(1-\Delta^2) - U^+(1-\Delta) + U^-(1+\Delta)}{A} \tag{19}$$

$$R^\pm = \frac{2G_0^\pm}{aC_\infty} + 6m^\pm\left(\frac{G_0^\pm}{aC_\infty} \pm \frac{\tilde{\zeta}}{\kappa a}\right) \tag{20}$$

$$U^\pm = \frac{48m^\pm}{\kappa a}\ln\left(\cosh\frac{\tilde{\zeta}}{4}\right) \tag{21}$$

$$m^\pm = \frac{2\epsilon_e}{3\eta D^\pm}\left(\frac{kT}{e}\right)^2 \tag{22}$$

$$G_0^\pm = \frac{2C_\infty}{\kappa}(e^{\mp\tilde{\zeta}/2} - 1) \tag{23}$$

$$\kappa = \sqrt{\frac{2e^2C_\infty}{kT\epsilon_e}} \tag{24}$$

$$\tilde{\zeta} = \frac{e\zeta}{kT} \tag{25}$$

Conductivity Increment. For low particle concentrations, the conductivity and the permittivity of the suspension are given by the well-known expressions[1]

$$k(\omega) = k_e + 3pk_e\left\{\mathrm{Re}[K_d(\omega)] - \frac{\omega\epsilon_e}{k_e}\mathrm{Im}[K_d(\omega)]\right\} \equiv k_e + p\Delta k(\omega) \tag{26}$$

$$\epsilon(\omega) = \epsilon_e + 3p\epsilon_e\left\{Re[K_d(\omega)] + \frac{k_e}{\omega\epsilon_e}\mathrm{Im}[K_d(\omega)]\right\} \equiv \epsilon_e + p\Delta\epsilon(\omega) \tag{27}$$

where

$$k_e = \frac{e^2 C_\infty}{kT}(D^+ + D^-) \tag{28}$$

is the conductivity of the electrolyte solution, p is the volume concentration of the suspended particles, while $\Delta k(\omega)$ and $\Delta\epsilon(\omega)$ are the conductivity and permittivity increments.

In view of the comment given above, eq 12, the low-frequency conductivity increment should neither be measured nor calculated using an applied DC electric field since, in this case, the measurement cell is acted upon by a macroscopic concentration gradient in addition to the electric potential gradient.[22] We calculated, therefore, the conductivity increment for an AC electric field considering a frequency value that is so low (10^{-2} Hz) that the resulting $\Delta k(0)$ value is frequency independent.

The results obtained are presented in Figure 1, panels a and b, as functions of the parameter Δ. Obviously, not all of the $-1 \le \Delta \le 1$ range is attainable in practice. However, substantial departures from $\Delta = 0$ are commonplace: $\Delta \cong \pm 0.2$ for NaCl, $\Delta \cong \pm 0.3$ for AcCl, $\Delta \cong \pm 0.6$ for NaOH, $\Delta \cong \pm 0.66$ for HCl, where the double sign corresponds to the two possible signs of the suspended particle.

The parameter values are given in Table 1. Note that, in all of the figures, the average value of the diffusion coefficients of the two types of ions is kept constant. Therefore, when the Δ parameter increases, D^- increases while D^+ decreases, keeping constant the electrolyte solution conductivity.

Figure 1a shows the expected dependence of the conductivity increment on the ζ potential: negative values for low ζ and increasingly positive ones for high ζ. The agreement between the theoretical and the numerical results is very good for low values of the ζ potential (taking into account the rather small value of $\kappa a = 10.4$) but becomes worse with higher values of ζ. This is a known behavior[23] with no obvious explanation since the theory makes no assumptions concerning the ζ potential value.

Figure 1b shows the dependence of the conductivity increment on the electrolyte concentration. The agreement between theoretical and numerical results is excellent for the highest concentration ($\kappa a = 104$) for which the curves actually overlap and reasonable for the middle one ($\kappa a = 10.4$). For the lowest concentration ($\kappa a = 1.04$), the theory cannot be used. The very high values of the conductivity increment appearing at very low concentrations are due to the dipolar coefficient value, which increases by orders of magnitude for very small κa.[24,25] This behavior is related to the growth of the effective radius of the particle for $\kappa a \ll 1$.

Figure 1, panels a and b, also shows a strong dependence on the parameter Δ: the conductivity increment strongly increases with the counterion mobility at constant conductivity. This behavior can be interpreted in terms of the low-frequency dipolar coefficient, eq 26. In a DC field, the electrolyte solution outside the double layer is electroneutral, so that this coefficient does not explicitly depend on Δ

$$K_{\text{dstatic}} = \frac{(R^+ - 1)}{2(R^+ + 2)} + \frac{(R^- - 1)}{2(R^- + 2)} + \frac{3(R^+ - R^-)\left[\dfrac{U^+}{2(R^+ + 2)} - \dfrac{U^-}{2(R^- + 2)}\right]}{(R^+ + 2)(R^- + 2 - U^-) + (R^- + 2)(R^+ + 2 - U^+)} \tag{29}$$

The implicit dependence is relatively weak, since it only appears through the parameter $m^\pm$ that is related to the convective fluid flow.

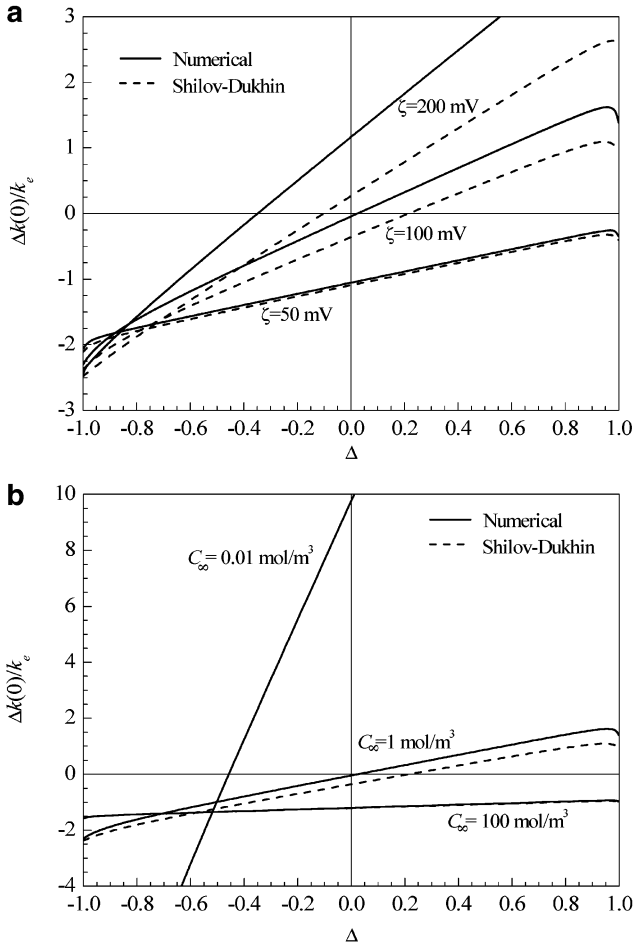

Figure 1. (a) Dependence of the conductivity increment, defined in eq 26, on the parameter Δ, eq 10, calculated for the indicated values of the ζ potential. The remaining parameters are given in Table 1. Numerical results (full lines) and theoretical predictions of the Shilov−Dukhin model (dashed lines). (b) As for panel a but calculated for the indicated values of the electrolyte solution concentration.

TABLE 1: Parameter Values Used in the Numerical and Analytical Calculations

	all the figures					
	$a = 100$ nm			$\epsilon_e = 78.54\ \epsilon_0$		$T = 273$ K
	$(D^+ + D^-)/2 = 2 \times 10^{-9}$ m² s⁻¹			$\eta = 8.094 \times 10^{-4}$ poise		
	a panels			b panels		
ζ [mV]	50	100	200	100		
C_∞ [mol m^{-3}]	1			0.01	1	100
κa	10.4			1.04	10.4	104
k_e [S m^{-1}]	0.015			0.00015	0.015	1.5

However, in a low-frequency AC field, a volume charge density builds up outside the double layer if $\Delta \neq 0$, which contributes to the dipolar coefficient, eq 12. It is well-known that the sign of $K_c(0)$ is determined by the sign of the ζ potential, being negative (positive) for positively (negatively) charged particles. Therefore, for positively (negatively) charged particles, $K_d(0) > K_{\text{dstatic}}$ when Δ is positive (negative). Combining this conclusion with definition 10 shows that, irrespective of the sign of ζ, $K_d(0) > K_{\text{dstatic}}$ when the diffusion coefficient of counterions is higher than that of co-ions.

Since the conductivity increment is proportional to the low-frequency limit of the dipolar coefficient, eq 26, its analytical expression is proportional to, eq 15

$$K_d(0) = \frac{(R^+ - 1)(1 - \Delta)}{2(R^+ + 2)} + \frac{(R^- - 1)(1 + \Delta)}{2(R^- + 2)} + \frac{3(R^+ - R^-)\left[\frac{U^+(1 - \Delta)}{2(R^+ + 2)} - \frac{U^-(1 + \Delta)}{2(R^- + 2)}\right]}{(R^+ + 2)(R^- + 2 - U^-) + (R^- + 2)(R^+ + 2 - U^+)} \quad (30)$$

which explicitly depends on Δ, increasing with this parameter. The sharp decrement appearing for extreme values of Δ is due to the contribution of convective flow to the surface conductivity that vanishes for these limits, as will be later discussed.

Electrophoretic Mobility. The considered theoretical model was already used by Dukhin and Semenikhin to calculate the electrophoretic mobility.[26] Unfortunately, the published result is limited to the case $\Delta = 0$, so that it cannot be used to analyze the dependencies discussed in this work. However, a general formula can be easily deduced considering a potential fluid flow outside the double layer

$$\vec{v} = -\nabla\Phi_v \quad (31)$$

$$\nabla^2\Phi_v = 0 \quad (32)$$

Using the thin double layer approximation, the corresponding boundary conditions, valid just outside the double layer, are

$$v_r = 0 \quad (33)$$

$$v_\theta = K_v \sin\theta \quad (34)$$

where the coefficient K_v can be calculated as the sum of the electroosmotic

$$v_{eo} = \frac{\epsilon_e \zeta}{\eta}\nabla_\theta \delta\Phi \quad (35)$$

and capillary osmotic

$$v_{co} = -\frac{4\epsilon_e}{\eta}\left(\frac{kT}{e}\right)^2 \ln\left(\cosh\frac{\tilde{\zeta}}{4}\right)\nabla_\theta \frac{\delta(C^+ + C^-)}{2C_\infty} \quad (36)$$

contributions. Since K_v is proportional to the electrophoretic velocity $v_p = 2K_v/3$, the final expression for the dimensionless electrophoretic mobility is

$$\mu = \frac{3e\eta v_p}{2kT\epsilon_e E} = \tilde{\zeta} - \tilde{\zeta}(K_d + K_c\Delta) + 4K_c \ln\left(\cosh\frac{\tilde{\zeta}}{4}\right) \quad (37)$$

The four addends in the right-hand side of this expression have a rather straightforward interpretation. The first three correspond to the electroosmotic velocity along a charged surface with potential ζ, which are induced by (a) the applied electric field, (b) the dipolar field of the particle, and (c) the field produced by the volume charge density outside the double layer. The fourth corresponds to the capillary osmotic contribution that is due to the electrolyte concentration gradient along the charged surface of the particle. Because of this gradient, the thickness of the double layer ceases to be uniform leading to a tangential gradient of the pressure and a tangential electric field inside the double layer, which contribute to the tangential fluid velocity.

Figure 2a represents the dimensionless electrophoretic mobility as a function of the parameter Δ, calculated for three different ζ potential values. The numerical results are compared to the theoretical ones calculated using eq 37 and to the expression

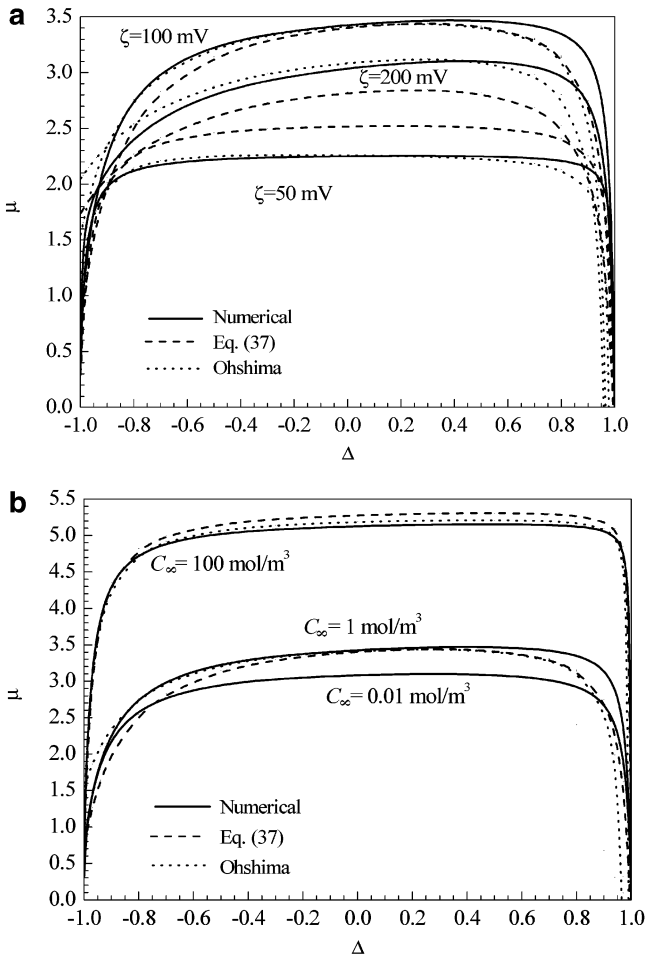

Figure 2. (a) Dependence of the dimensionless electrophoretic mobility, defined by the first equality in eq 37, on the parameter Δ, eq 10, calculated for the indicated values of the ζ potential. The remaining parameters are given in Table 1. Numerical results (full lines), eq 37 based on the Shilov−Dukhin model (dashed lines), Ohshima's[6] equation (dotted lines). (b) As for panel a but calculated for the indicated values of the electrolyte solution concentration.

deduced by Ohshima et al.[6] Although both formulas qualitatively reproduce the numerical data, Ohshima's equation is clearly more precise for moderate values of Δ. However, for extreme values of this parameter, only the expression based on the Shilov−Dukhin model exhibits the correct limiting behavior.

The three curves show the well-known nonmonotonic dependence of the mobility on the ζ potential.[9] They also show a very weak dependence on Δ for moderate values of this parameter. The reason for this is that the electroosmotic contribution to the electrophoretic mobility, determined by the total tangential electric field in the double layer, is proportional to the static value of the dipolar coefficient, eq 12, which does not explicitly depend on Δ, eq 29. On the other hand, the capillary osmotic contribution to the electrophoretic mobility, eq 37, is proportional to the field-induced electrolyte concentration change, eq 14. Its value is determined by the difference between the ratios of the counterion and co-ion transport parameters in the double layer and in the bulk electrolyte solution. These ratios are mainly determined by the equilibrium ion concentrations inside the double layer (which depend on the ζ potential) and in the bulk. However, they do not depend on the diffusion coefficient values since, for each ion type, both the surface conductivity and the bulk conductivity are proportional to the corresponding diffusion coefficient. This behavior is reflected in the analytical expression

$$K_c(0) = \frac{R^+ - 1}{2(R^+ + 2)} - \frac{R^- - 1}{2(R^- + 2)} + \frac{3(R^+ - R^-)\left[\frac{U^+}{2(R^+ + 2)} + \frac{U^-}{2(R^- + 2)}\right]}{(R^+ + 2)(R^- + 2 - U^-) + (R^- + 2)(R^+ + 2 - U^+)} \quad (38)$$

which does not explicitly depend on the parameter Δ.

Finally, Figure 2a shows a very strong dependence on Δ for extreme values of this parameter. The reason for this is that the electrophoretic mobility must vanish for $\Delta = \pm 1$, that is when the mobility of counterions or co-ions vanishes. This requirement can be deduced from eq 1, which shows that the flow of ions with vanishing diffusion coefficient is equal to their concentration multiplied by the fluid velocity. Taking the divergence of this equation and combining the result with the incompressibility condition (4) shows that the fluid velocity must vanish wherever the equilibrium concentration is not uniform. Qualitatively, this means that it is not possible to move the fluid with respect to a suspended particle while keeping a nonuniform ion distribution around it, without moving the ions with respect to the fluid.

Figure 2b shows the results of the electrophoretic mobility calculated for three different electrolyte concentration values. The curves show the well-known monotonic dependence on the concentration or rather the κa value.[9] The agreement between the two theoretical results and the numerical values is quite good for the two highest concentrations ($\kappa a = 104$ and 10.4), whereas both analytical expressions cannot be used for the lowest one ($\kappa a = 1.04$). Furthermore, the agreement generally worsens for high $|\Delta|$, which is probably due to the use of the hypothesis of approximate electroneutrality in the case of eq 37, based on the Shilov−Dukhin model.

Permittivity Increment. Figure 3, panels a and b, represents the dependence of the permittivity increment, eq 27, on the parameter Δ, for different values of the ζ potential and of the electrolyte concentration. The theoretical results reproduce surprisingly well the rather complicated features of the numerical data. Most notable is the behavior for very high Δ values, where the curves show a behavior that could easily be interpreted as a numerical artifact. Quantitatively, the biggest disagreement corresponds, as for Figure 1a, to the highest ζ potential value.

The strong dependence of the permittivity increment on Δ can be interpreted considering the dependence of the imaginary part of the dipolar coefficient on this parameter since, according to eq 27, $\Delta\epsilon(0)$ is proportional to $\lim_{\omega\to 0}\{\mathrm{Im}[K_d(\omega)]/\omega\}$, except for very low values of the ζ potential. This limit is determined by two main factors:

1. The amplitude of the imaginary part of the dipolar coefficient, which is proportional to the difference between the high and the low-frequency limits of the dipolar coefficient, $K_{d\infty} - K_d(0)$. Both addends explicitly depend on the parameter Δ: when the counterion mobility is increased, the value of $K_{d\infty}$ increases, eq 18, since it is determined by the surface conductivity (roughly proportional to the counterion mobility) divided by the electrolyte solution conductivity (that is kept constant). The dependence of $K_d(0)$ on Δ was already discussed. The analytic expression for the difference can be written using eq 15

$$K_{d\infty} - K_d(0) = K_c(0)\frac{(R^+ - R^-)(1 - \Delta^2) - U^+(1 - \Delta) + U^-(1 + \Delta)}{R^+(1 - \Delta) + R^-(1 + \Delta) + 4} \quad (39)$$

where $K_c(0)$ does not explicitly depend on Δ, eq 38. This dependence of the imaginary part of the dipolar coefficient is responsible for the linear decrease of the permittivity increment with Δ, valid for low values of $|\Delta|$, Figure 3, panels a and b.

2. The characteristic time of the low-frequency dielectric dispersion. The permittivity increment is proportional to the corresponding characteristic time, which is the reason of the huge amplitude values that can be attained by this dispersion. This dependence can be analytically obtained calculating the low-frequency limit of the imaginary part of $K_d(\omega)$, eqs 14 and 15, which is proportional to W^2. This shows that the permittivity increment should be inversely proportional to D_{ef}, eqs 8 and 9, which decreases with $|\Delta|$ since the characteristic time of the dispersion is determined by the ion with the lesser mobility, irrespective of its sign. This dependence of the imaginary part of the dipolar coefficient is responsible for the strong increase of the permittivity increment with $|\Delta|$, valid for large values of this parameter, Figure 3, panels a and b.

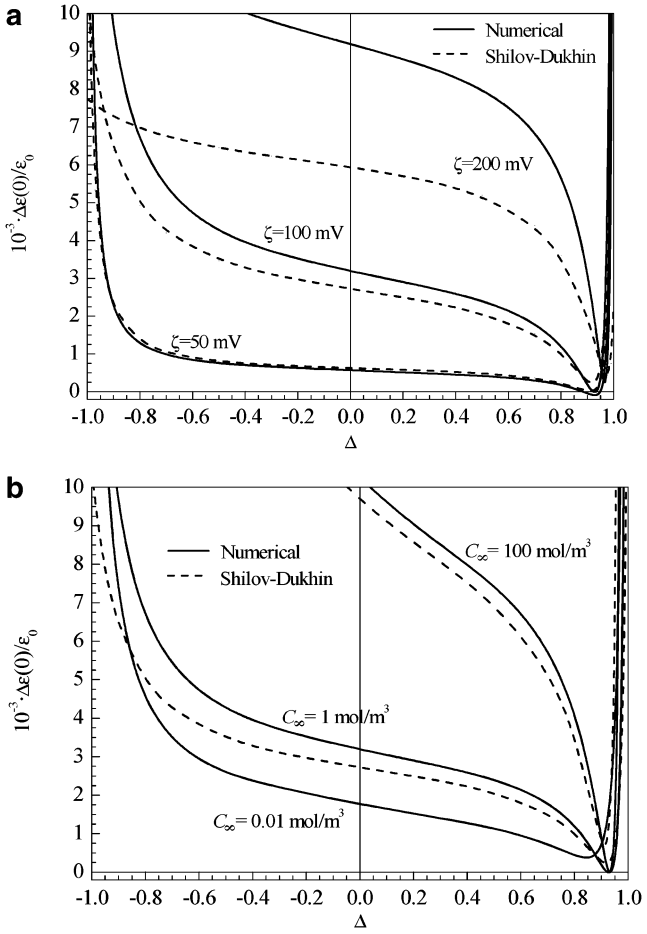

Figure 3. (a) Dependence of the permittivity increment, defined in eq 27, on the parameter Δ, eq 10, calculated for the indicated values of the ζ potential. The remaining parameters are given in Table 1. Numerical results (full lines) and theoretical predictions of the Shilov−Dukhin model (dashed lines). (b) As for panel a but calculated for the indicated values of the electrolyte solution concentration.

Conclusion

In this work, the dependence of some electrokinetic and dielectric properties of colloidal suspensions on the difference between the counterion and co-ion mobilities has been analyzed. Although this dependence is predicted by existing approximate analytical expressions, such a study was never performed, to our knowledge. Moreover, no numerical results covering a broad range of system parameters were available. A reason for this is

that, when the counterion and co-ion mobility values differ from one another, an applied AC field induces electric charge densities that extend to great distances beyond the double layer,[16] which greatly increases the difficulties of the numerical calculations. In the present case, the network simulation method made it possible to solve the problem considering the full range of counterion and co-ion mobilities and for the very low frequencies required for the calculation of zero-frequency (as opposed to static) properties, such as the conductivity and the permittivity increments.

Calculations performed for different ζ potential and electrolyte concentration values show that the three investigated parameters have very different dependencies on the counterion mobility. Keeping constant the κa and the electrolyte solution conductivity values, the conductivity increment strongly increases, the electrophoretic mobility barely changes, whereas the permittivity increment strongly decreases. These simple trends, valid for small values of the Δ parameter, are well reproduced by the analytical expressions, although quantitative agreement is only attained for high κa and moderate ζ potential values. They can be interpreted in terms of the dependencies on the Δ parameter of the low-frequency limit of the dipolar coefficient, of the static value of the dipolar coefficient together with the low-frequency limit of the electrolyte concentration change, and of the amplitude of the imaginary part of the dipolar coefficient.

These simple dependencies cease to be valid when the counterion and co-ion mobility values strongly differ: the electrophoretic mobility diminishes tending to zero for $\Delta \rightarrow \pm 1$, whereas the permittivity increment sharply increases. Rather unexpectedly, this behavior is also qualitatively reproduced by the analytical expressions, despite the use of the hypothesis of approximate electroneutrality outside the double layer, in the case of the Shilov−Dukhin model. It can be interpreted in terms of the dependencies on the Δ parameter of the fluid velocity inside the double layer and of the characteristic time of the low-frequency dielectric dispersion.

Acknowledgment. Financial support by Ministerio de Ciencia y Tecnología, Spain, under Project BFM2003-4856, and by the Consejo de Investigaciones de la Universidad Nacional de Tucumán, Agencia Nacional de Promoción Científica y Tecnológica, and Consejo Nacional de Investigaciones Científicas y Técnicas, Argentina, is gratefully acknowledged.

References and Notes

(1) Dukhin, S. S.; Shilov, V. N. *Dielectric Phenomena and the Double Layer in Disperse Systems and Polyelectrolytes*; Wiley: New York, 1974.
(2) Lyklema, J. *Fundamentals of Interface and Colloid Science*; Academic Press: New York, 1995.
(3) Delgado, A. V. *Interfacial Electrokinetics and Electrophoresis*; Marcel Dekker: New York, 2002.
(4) O'Brien, R. W. *Adv. Colloid Interface Sci.* **1982**, *16*, 281
(5) Fixman, M. *J. Chem. Phys.* **1983**, *78*, 1483.
(6) Ohshima, H.; Healy, T. W.; White L. R. *J. Chem. Soc., Faraday Trans. 2* **1983**, *79*, 1613.
(7) Grosse, C.; Shilov, V. N. *J. Colloid Interface Sci.* **1999**, *211*, 160.
(8) Wiersema, P. H.; Loeb, A. L.; Overbeek, J. Th. G. *J. Colloid Interface Sci.* **1966**, *22*, 70.
(9) O'Brien, R. W.; White, L. R. *J. Chem. Soc., Faraday Trans.* 2 **1978**, *74*, 1607.
(10) DeLacey, E. H. B.; White, L. R. *J. Chem. Soc., Faraday Trans. 2* **1981**, *77*, 2007.
(11) Mangelsdorf, C. S.; White, L. R. *J. Chem. Soc., Faraday Trans.* **1992**, *88*, 3567.
(12) López-García, J. J.; Horno, J.; González-Caballero, F.; Grosse, C.; Delgado, A. V. *J. Colloid Interface Sci.* **2000**, *228*, 95.
(13) Shilov, V. N.; Delgado, A. V.; Gonzalez-Caballero, F.; Grosse, C. *Colloids Surf. A* **2001**, *192*, 253.
(14) Arroyo, F. J.; Delgado, A. V.; Carrique, F.; Jiménez, M. L.; Bellini, T.; Mantegazza, F. *J. Chem. Phys.* **2002**, *114*, 10973.
(15) Grosse, C.; López-García, J. J.; Horno, J. *J. Phys. Chem. B* **2004**, *108*, 8397.
(16) López-García, J. J.; Grosse, C.; Horno, J. *J. Phys. Chem. B* **2005**, *109*, 5808.
(17) López-García, J. J.; Grosse, C.; Horno, J. *J. Colloid Interface Sci.* **2003**, *265*, 327.
(18) López-García, J. J.; Grosse, C.; Horno, J. *J. Colloid Interface Sci.* **2003**, *265*, 341.
(19) Moya, A. A.; Horno, J. *J. Phys. Chem. B* **1999**, *103*, 10791.
(20) López-García, J. J.; Horno, J. In *Network Simulation Method*; Horno, J., Ed.; Research Signpost: Trivandrum, 2002.
(21) Grosse, C.; Shilov, V. N. *J. Phys. Chem.* **1996**, *100*, 1771.
(22) López-García, J. J.; Horno, J.; Grosse, C.; Delgado, A.; Shilov, V. N. *J. Colloid Interface Sci.* **2001**, *241*, 98.
(23) Pedrosa, S. E.; Grosse, C. *J. Colloid Interface Sci.* **1999**, *219*, 37.
(24) Grosse, C.; Pedrosa, S. E.; Shilov, V. N. *J. Colloid Interface Sci.* **2002**, *251*, 304.
(25) Grosse, C.; Pedrosa, S. E.; Shilov, V. N. *J. Colloid Interface Sci.* **2003**, *265*, 197.
(26) Dukhin, S. S.; Semenikhin, N. M. *Koll. Zh.* **1970**, *32*, 366.
(27) Landau, L. D.; Lifshitz, E. M. *Mecánica de Fluidos*; Reverté: Barcelona, 1991.